Cancer Cell
Article

In Vivo-Restricted and Reversible Malignancy Induced by Human Herpesvirus-8 KSHV: A Cell and Animal Model of Virally Induced Kaposi's Sarcoma

Agata D'Agostino Mutlu,[1,7] Lucas E. Cavallin,[1,4,7] Loïc Vincent,[2] Chiara Chiozzini,[1] Pilar Eroles,[1] Elda M. Duran,[4] Zahra Asgari,[1] Andrea T. Hooper,[2] Krista M.D. La Perle,[3] Chelsey Hilsher,[5] Shou-Jiang Gao,[6] Dirk P. Dittmer,[5] Shahin Rafii,[2] and Enrique A. Mesri[1,4,*]

[1] Laboratory of Viral Oncogenesis, Division of Hematology-Oncology, Department of Medicine
[2] Howard Hughes Medical Institute, Department of Genetic Medicine
[3] Department of Pathology and Laboratory Medicine
Weill Medical College of Cornell University, New York, NY 10021, USA
[4] Program in Viral Oncology, Department of Microbiology & Immunology and Sylvester Comprehensive Cancer Center, University of Miami Miller School of Medicine, Miami, FL 33136, USA
[5] Department of Microbiology and Immunology and Lineberger Comprehensive Cancer Center, University of North Carolina, Chapel Hill, NC 27599, USA
[6] Departments of Pediatrics and Microbiology and Children's Cancer Research Institute, University of Texas Health Science Center, San Antonio, TX 78229, USA
[7] These authors contributed equally to this work.
*Correspondence: emesri@med.miami.edu
DOI 10.1016/j.ccr.2007.01.015

SUMMARY

Transfection of a Kaposi's sarcoma (KS) herpesvirus (KSHV) Bacterial Artificial Chromosome (KSHVBac36) into mouse bone marrow endothelial-lineage cells generates a cell (mECK36) that forms KS-like tumors in mice. mECK36 expressed most KSHV genes and were angiogenic, but they didn't form colonies in soft agar. In nude mice, mECK36 formed KSHV-harboring vascularized spindle cell sarcomas that were LANA+/podoplanin+, overexpressed VEGF and Angiopoietin ligands and receptors, and displayed KSHV and host transcriptomes reminiscent of KS. mECK36 that lost the KSHV episome reverted to nontumorigenicity. siRNA suppression of KSHV vGPCR, an angiogenic gene upregulated in mECK36 tumors, inhibited angiogenicity and tumorigenicity. These results show that KSHV malignancy is in vivo growth restricted and reversible, defining mECK36 as a biologically sensitive animal model of KSHV-dependent KS.

INTRODUCTION

Human herpesvirus-8 or Kaposi's sarcoma-associated herpesvirus (KSHV) is associated with three AIDS-related malignancies: Kaposi's sarcoma (KS) (Boshoff and Weiss, 1998; Chang et al., 1994; Ganem, 2006), Multicentric Castlemans disease (Dupin et al., 1999), and primary effusion lymphoma (Cesarman et al., 1995). In HIV-infected individuals, predominantly in the male homosexual population, the incidence of KS dramatically increases and can manifest as an advanced disseminated cancer with increased morbidity and mortality (Gallo, 1998). The development of pathogenesis-based therapies is important for improving current KS treatments (Pantanowitz and Dezube, 2004).

SIGNIFICANCE

Kaposi's sarcoma (KS) herpesvirus (KSHV) is the etiologic agent of KS, an angiogenic spindle cell sarcoma associated with AIDS. The mechanisms driving KSHV carcinogenesis could be uncovered through reproduction of KS by KSHV infection of normal cells. Our results defining this cell and animal model of KS show that KSHV-induced neoplasia is reversible, KSHV dependent, and in vivo restricted. Upregulation of KSHV genes, such as the proangiogenic vGPCR, under in vivo growth conditions provides a selective advantage to KSHV-harboring cells and leads to episome maintenance and tumorigenesis. Thus, mECK36 tumors are phenotypic, molecular, and viral surrogates of KS that are suitable for analyzing the role of viral and host genes in KS pathogenesis, and for preclinical testing of anti-KS drugs.

KS presents itself as multifocal lesions in the skin, lungs, and gastrointestinal tract (Safai et al., 1985). It is characterized by intense VEGF-mediated angiogenesis, spindle cell proliferation, and erythrocyte extravasation (Gallo, 1998; Safai et al., 1985). There are many key unanswered issues in KS pathogenesis that are matters of controversy and intense research: (1) the neoplastic nature of KS, (2) the identity of the normal cell type that upon infection with KSHV becomes a malignant KS spindle cell, (3) the connection between KSHV gene expression and the KS phenotype, and (4) the relationship between KSHV biology and other KS cofactors, such as immunosuppression, HIV infection, and sexual transmission. Primary to answering these questions is the development of an experimental model of KSHV infection that reproduces the main pathogenic phenotypes of KS in vitro and in animals.

While spindle cells are generally considered the tumor cell in KS lesions, their origin and true malignant nature are controversial, because they lack many features of neoplastic cells such as aneuploidy, tumorigenicity (Gallo, 1998), or clonality (Gill et al., 1998). KS spindle cells express phenotypic markers that belong to many cell lineages, including endothelium, smooth muscle cells, macrophages, and hematopoietic cells (Boshoff and Weiss, 2002; Gallo, 1998). Since KS could present itself as a multifocal disease, and KS spindle cells express the hematopoietic stem cell marker CD34, it has been proposed that the KS progenitor cell is a circulating cell of the hematopoietic endothelial lineage (Barozzi et al., 2003; Boshoff and Weiss, 2002; Browning et al., 1994). Spindle cells in the lesions express markers characteristic of the lymphatic endothelial cell (EC) lineage, such as LYVE-1, podoplanin, and VEGF-R3. It has been recently suggested that they originate from lymphatic endothelium (Dupin et al., 1999; Skobe et al., 1999), transdifferentiated vascular endothelium, or a common EC precursor (Hong et al., 2004; Wang et al., 2004).

It is now well established that KSHV is an etiologic cofactor strictly necessary for KS (Boshoff and Weiss, 1998; Chang et al., 1994; Ganem, 2006), indicating that KSHV genetic expression is responsible for the KS angiogenic phenotype. Although the KSHV genome encodes for genes that can induce cell transformation (Gao et al., 1997; Lee et al., 1998; Wang et al., 2006), immune deregulation (Moore et al., 1996; Nicholas et al., 1997), and angiogenesis activation (Aoki et al., 1999; Bais et al., 1998, 2003; Boshoff et al., 1997; Montaner et al., 2003; Yang et al., 2000), KSHV infection leads to KS in limited circumstances.

Since KSHV is an endothelial-tropic virus, several KSHV-infection models using ECs have been described (Ciufo et al., 2001; Flore et al., 1998; Hong et al., 2004; Lagunoff et al., 2002; Moses et al., 1999; Naranatt et al., 2004; Wang et al., 2004). In contrast to the oncogenicity and tumorigenicity of its viral genome, KSHV infection of ECs leads to the induction of KS markers, a spindle cell phenotype, and signs of transformation, but it does not result in the acute angiogenicity and tumorigenicity characteristic of KSHV-infected spindle cells in lesions. This suggests that key oncogenic events are not recapitulated in the KSHV-infected EC cultures. Plausible explanations for this are the tendency for either latency or productivity of the in vitro infections, the possibility that terminally differentiated ECs may not be suitable KS progenitors, or that in vivo growth conditions not mimicked in culture are essential for KSHV oncogenicity.

Here, we report that bacterial artificial chromosome (KSHVBac36) transfection of normal mouse bone marrow endothelial-lineage cells induces an angiogenic phenotype and KS-like, KSHV-dependent tumorigenicity. This identifies a cell population containing putative KS progenitors and establishes a KS model with the following characteristics: (1) the pathological phenotype is a consequence of KSHV gene expression in normal progenitor cells subjected to in vivo growth conditions, (2) the histopathologic phenotype of the tumors resembles KS lesions, and (3) the model is suitable for genetic analysis of viral pathogenesis.

RESULTS

Bac36 Transfection of Mouse Bone Marrow Endothelial Hematopoietic Cells Leads to KSHV Latent and Lytic Gene Expression

To create a mouse model of KS, we used as targets of KSHV infection mouse bone marrow adherent-cell preparations enriched in endothelial-lineage cells (mECs) containing mature ECs, their progenitors, and proangiogenic hematopoietic cells (Boshoff and Weiss, 2002; Rafii and Lyden, 2003). To be able to select and track infected cells, we transfected mECs with KSHVBac36, which encodes the full infectious KSHV genome in a hygromycin (Hyg)-resistant and EGFP-encoding bacterial artificial chromosome (KSHVBac36) (Zhou et al., 2002). mECs transfected with the Bac backbone vector (mEC-V) were used as control. After 3 weeks of Hyg selection, both KSHVBac36-transfected mECs (mECK36) and mEC-V formed contact-inhibited, stromal cell-like monolayers. We found that mECK36 cultures were over 95% EGFP+ (Figure 1A), indicating the presence of KSHVBac36. To determine if the EGFP+ cell population was infected by KSHV, we analyzed the expression of the latent genes LANA and Kaposin by immunofluorescence. As shown in Figures 1A and 1B, all EGFP+ mECK36 were positive for LANA and displayed the classic nuclear punctuated pattern produced by the tethering of KSHV episomes to the host chromosome (Ballestas et al., 1999). As shown in Figure 1C, mECK36 also stained for the latent oncogene Kaposin (Muralidhar et al., 1998) and displayed its characteristic perinuclear localization.

To estimate the integrity of the KSHV genome in mECK36, we performed real-time RT-PCR analysis for the entire KSHV transcriptome of mECK36 (Dittmer, 2003; Fakhari and Dittmer, 2002). We compared the expression pattern in the endothelial-lineage (mECK36) cells with non-KSHV targets (Bac36-transfected NIH 3T3 cells) (C.C., A.D.M., and E.A.M., unpublished data). mRNA levels were 218-fold higher (CV: 45…391, n = 100,

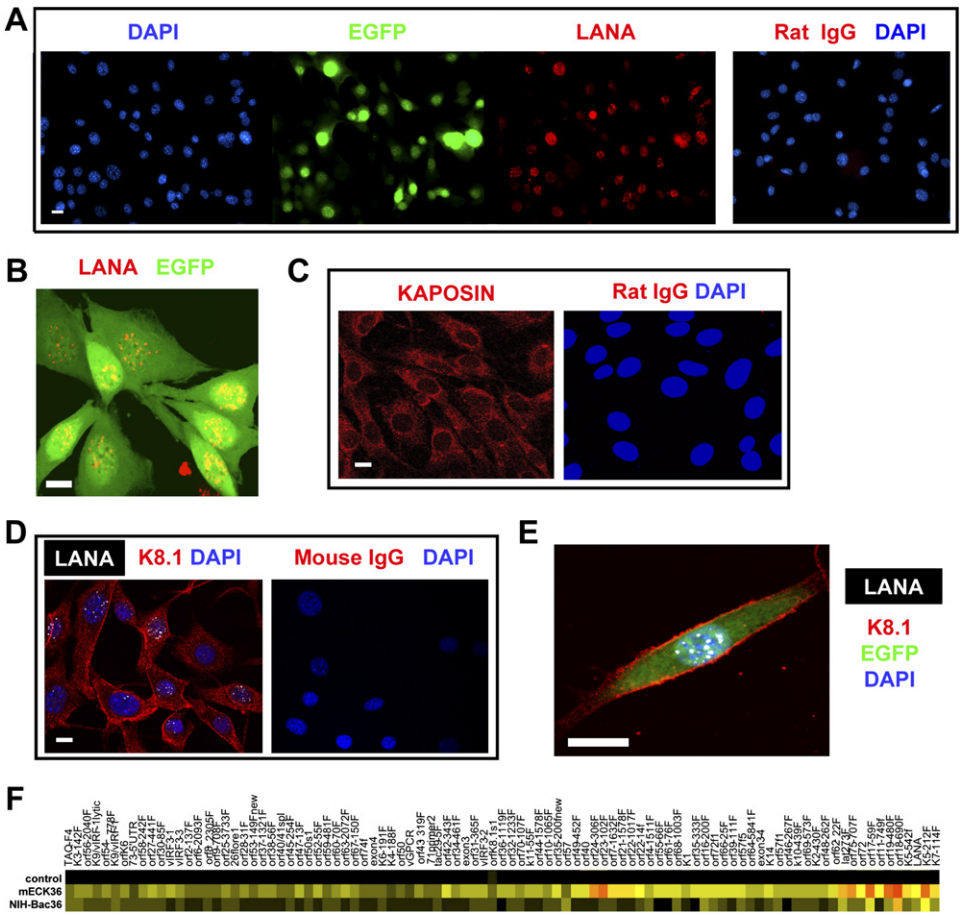

Figure 1. KSHVBac36 Transfection of Mouse Bone Marrow Endothelial Hematopoietic Cells Leads to KSHV Latent and Lytic Gene Expression

(A) Immunofluorescence staining of LANA.

(B) Confocal image showing punctuated LANA staining.

(C) Immunofluorescence staining of Kaposin.

(D) Immunofluorescence staining of K8.1 and LANA.

(E) Detailed confocal image of LANA and K8.1.

(F) Heatmap representation of real-time RT-PCR analysis for the entire KSHV transcriptome in Bac36KSHV-transfected cells. Ctrl, mock-transfected NIH 3T3 cells. Red indicates the highest, yellow indicates intermediate, and black indicates the lowest relative mRNA levels. The scale bar is 10 μM.

$p \leq 10^{-14}$) in mECK36 than in Bac36-transfected NIH 3T3 cells. In contrast, KSHV latent mRNAs (LANA, lat273f, orf72, Taq-F4, 73-5′UTR, orf72f1) were present at about equal levels, with a mean difference of 2.24-fold (CV: −1.04.5.51, n = 6, $p \leq 0.29$). This shows that mECK36 have increased lytic gene expression. All KSHV genes are expressed over background levels (Figure 1F), indicating that the KSHV transcriptome is complete in mECK36, further suggesting that the Bac has not undergone major deletions or translocations that would affect KSHV gene expression.

Although lytic gene transcription in mECK36 is abundant, they did not produce KSHV virions, as indicated by transmission electron microscopy analysis and the absence of a cytopathic effect (CPE) (data not shown). Double immunofluorescence staining for the latent antigen LANA and the late lytic antigen K8.1 shows a coexpression pattern (Figures 1D and 1E) in most of the cells, which, together with the mECK36 KSHV transcription profile, is indicative of an abortive lytic transcription status.

KSHVBac36-Transfected Bone Marrow Endothelial-Lineage Cells Are Angiogenic

The abortive lytic status of mECK36 is expected to be highly oncogenic, since it combines the expression of latent and lytic KSHV genes with transforming and angiogenesis-inducing potential. Both mEC-V and mECK36 became immortalized in culture and could be passaged infinitely (current passages > 50). Since murine cells express telomerase, they generally become immortalized as a consequence of cell culture shock (Sherr and DePinho, 2000). KSHV genes can upregulate telomerase expression (Knight et al., 2001); therefore, we tested telomerase activity in mEC-V and mECK36 and found

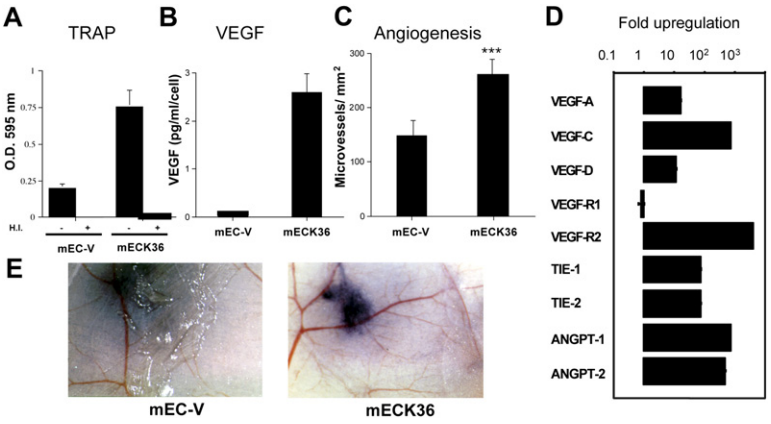

Figure 2. KSHVBac36 Transfection of mECs Induces an Angiogenic Phenotype

(A) ELISA-based Telomerase Repeat Amplification Protocol (TRAP) assay of mEC-V and mECK36. Bars indicate mean of duplicates ± SEM.

(B) VEGF secretion levels of mEC-V and mECK36. Bars indicate mean of duplicates ± SEM.

(C) Intradermal skin angiogenesis assay (see Experimental Procedures) of mEC-V and mECK36. The bar graphs show the mean microvessel density (vessels/mm^2) × 100 ± SEM. Total n (both flanks) = 10. (***$p < 0.05$).

(D) KSHVBac36-induced upregulation of angiogenic gene expression determined by real-time qRT-PCR. Bars represent mean fold increase (triplicates ± SEM) in mRNA levels between mECK36 and mECs.

(E) Appearance at a dissected inoculation site in the skin of a mouse injected with mECs or mECK36.

increased levels in mECK36 (Figure 2A). Transformed cells have increased telomerase expression; yet, the finding that mECK36 were contact inhibited suggested that they were not transformed. To identify transformed clones among the mECK36 population, we carried out an anchorage-independent growth assay in soft agar by using NIH 3T3 and RasV12-transformed NIH 3T3 cells as negative and positive controls, respectively. While 92% of the RasV12-transformed NIH 3T3 cells formed colonies in soft agar, neither mECK36, mEC-V, nor control NIH 3T3 cells formed colonies, suggesting that mECK36 are not transformed. To investigate KSHVBac36-induced angiogenicity, we determined VEGF secretion levels, mRNA expression of angiogenic markers, and skin angiogenicity in mEC-V and mECK36. As shown in Figures 2B–2E, KSHVBac36 transfection of mECs increased VEGF secretion levels, upregulated ligands and receptors of the VEGF and Angiopoietin family, and displayed a significantly increased ability ($p < 0.05$) to induce microvessel formation in mice skin. Taken together, these results indicate that KSHV expression in mECs induces an angiogenic phenotype.

KSHVBac36-Transfected Bone Marrow Endothelial Hematopoietic Cells Form KSHV-Infected Tumors that Resemble Kaposi's Sarcoma

Cell angiogenicity is key for tumor growth. To determine if mECK36 were tumorigenic in mice, they were injected subcutaneously in nude mice by using mEC-V as controls. We found that mECK36 formed solid tumors 3 weeks after injection, in contrast to mEC-V, which did not (Figures 3A–3C). Upon dissection, we found that the tumors were green-yellow, indicating a significant percentage of EGFP+ cells (Figure 3B). Tumors were analyzed in a blind fashion and were found to be "vascularized spindle cell sarcomas," which is the histological presentation of human KS tumors (Figure 3D). Advanced invasive KS often appears as multifocal lesions on the lungs and the gastrointestinal tract (Safai et al., 1985). To determine whether mECK36 could also induce invasive KS, we injected passage 30 cells

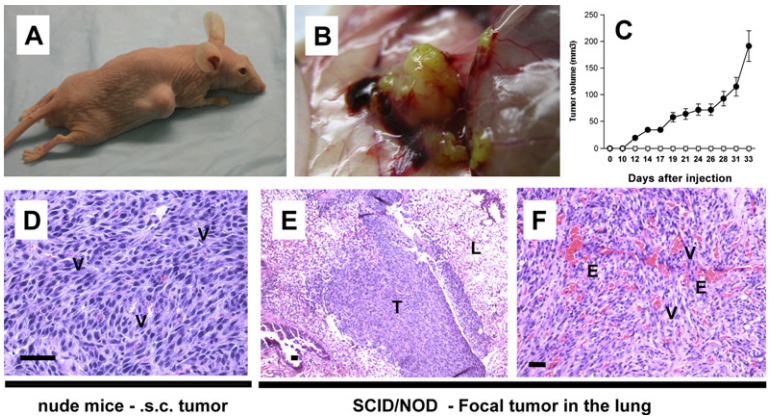

Figure 3. mECK36 Induce Vascularized Spindle Cell Sarcomas in Immunocompromised Mice

(A) Mice showing a subcutaneous mECK36 tumor 4 weeks after inoculation.

(B) Dissection site showing a green-yellow tumor (EGFP expression).

(C) Subcutaneous tumor growth in nude mice injected with mECK36 (closed circles) or mEC-V (open squares). Data indicate mean tumor size (n = 7) ± SEM.

(D) Microscopic image of a histological section of a mECK36 tumor stained with hematoxylin and eosin (H&E). V, microvessel.

(E) Image of a spindle cell sarcoma foci (T) growing in the lung (L) stained with H&E.

(F) Image of a spindle cell tumor in the lungs stained with H&E. E, blood extravasation; V, microvessel. The scale bar is 50 μM.

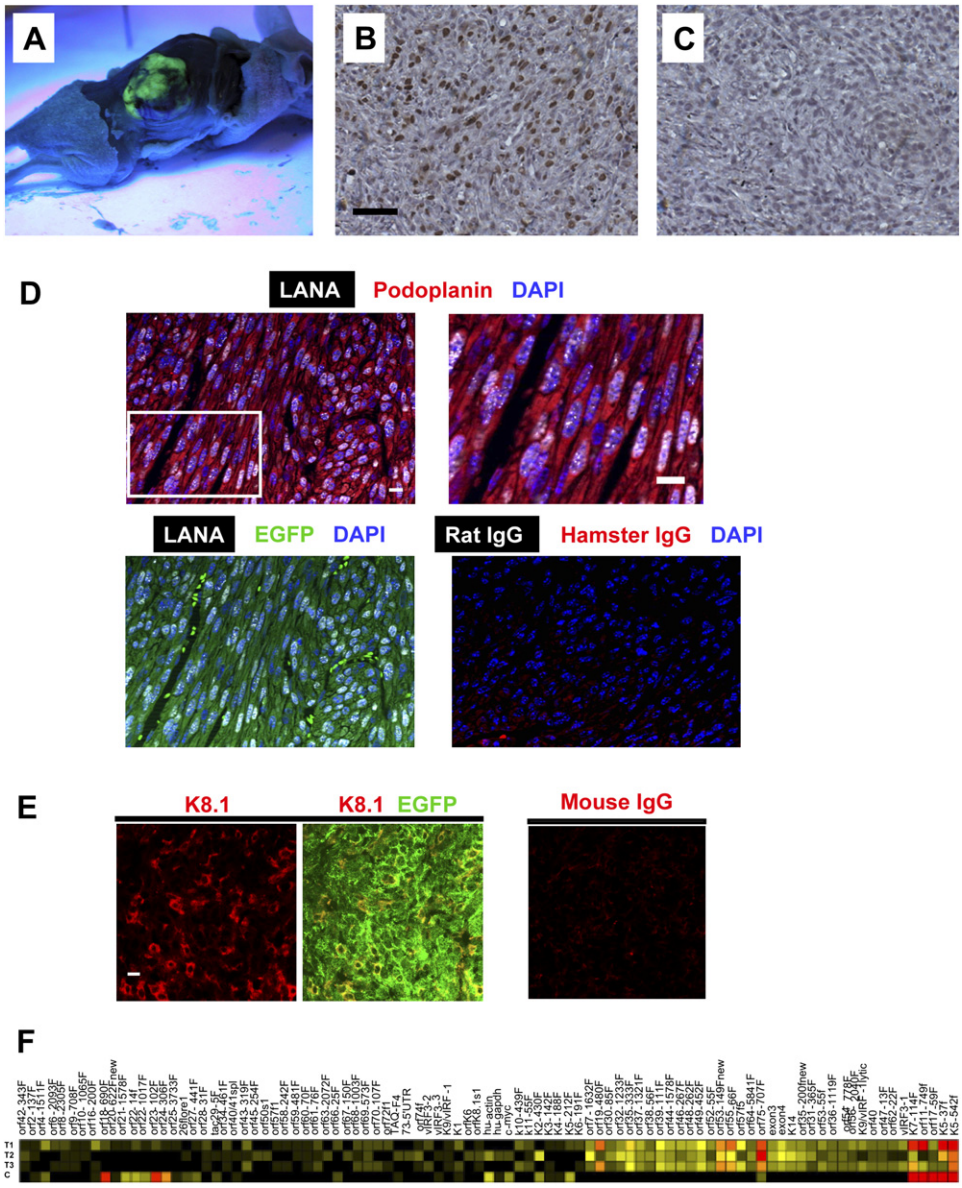

Figure 4. mECK36 Induce KSHV-Bearing Spindle Cell Sarcomas Resembling KS Tumors

(A) Dissected mouse showing subcutaneous fluorescent tumor observed under long-wave UV light.

(B) LANA immunohistochemistry of paraffin-embedded mECK36 tumors. The scale bar is 50 μM.

(C) Rat IgG control for LANA immuohistochemistry. The scale bar is 50 μM.

(D) Top left: confocal images showing podoplanin staining in the cytoplasm and LANA staining in the nucleus. Top right: higher-magnification image showing the speckled pattern of LANA immunofluorescence in podoplanin+ cells. Bottom left: colocalization of LANA with EGFP. Bottom right: an isotype-matched control. The scale bar is 10 μM.

(E) Confocal images showing K8.1 staining in the membrane (left) and colocalizing with EGFP (middle). (Right) Mouse IgG control. The scale bar is 10 μM.

(F) Heatmap representation of KSHV transcriptome in mECK36 tumors and mECK36 grown in culture quantified by using real-time qRT-PCR. C, mECK36 grown in culture; T1, T2, and T3, primary mECK36 tumors. Red indicates the highest, yellow indicates intermediate, and black indicates the lowest relative mRNA levels.

intravenously in irradiated SCID/NOD mice. A total of 3 months after injection, mECK36-injected animals were sick, while mEC-V-injected animals did not show any signs of ailment. Necropsy of mECK36-injected animals revealed multifocal, invasive spindle cell sarcoma lesions in lungs (9–20 foci per lung) (Figures 3E and 3F), a presentation reminiscent of advanced visceral KS.

The fact that subcutaneous tumors showed strong EGFP fluorescence (Figure 4A) indicated the presence of mECK36 in the tumors. Although mECK36 did not display

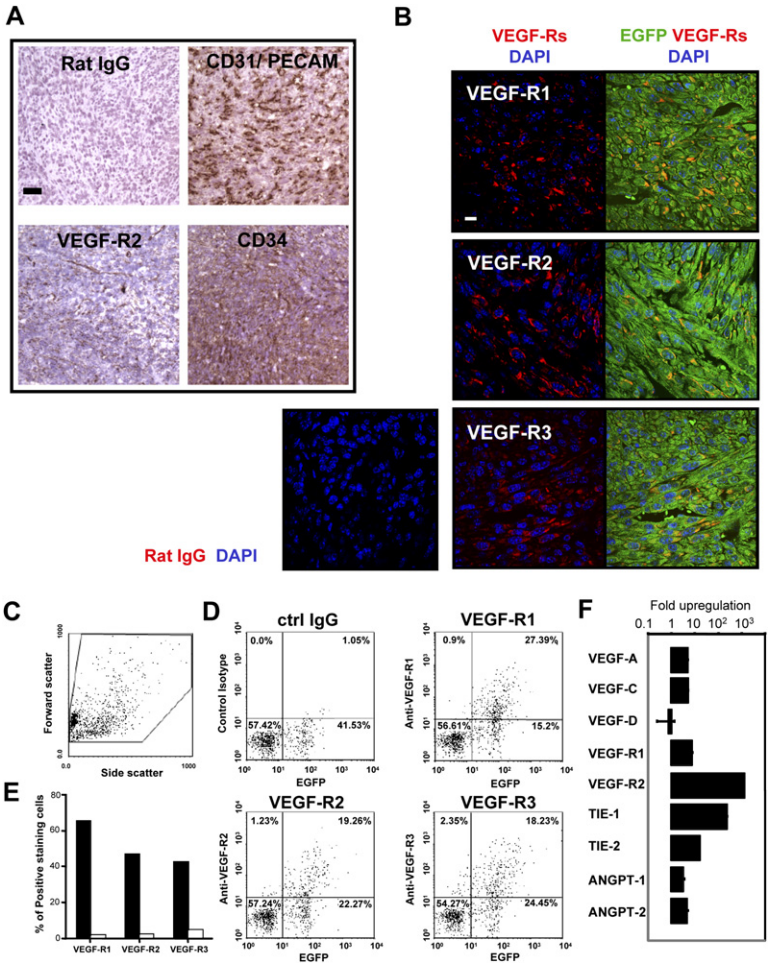

Figure 5. mECK36 Spindle Cell Sarcomas Express KS and Angiogenic Markers

(A) Frozen sections of tumors stained with indicated antibodies. The scale bar is 50 μM.

(B) Paraffin-embedded tissue sections stained with the indicated antibody and developed with Cy3-conjugated anti-IgG. The scale bar is 10 μM.

(C) Side and forward scatter of VEGF receptors on single-cell suspensions from mECK36 tumors by flow cytometry.

(D) Cells double positive for EGFP and indicated VEGFR from tumors in (C).

(E) Percentage of cells expressing VEGFR among the EGFP+ (black bars) and EGFR− (white bars) population.

(F) Upregulation of angiogenic gene expression in mECK36 tumors compared to cultured mECK36. Bars represent mean fold increase (triplicates ± SEM) in mRNA levels quantified by real-time qRT-PCR.

typical signs of cell transformation in vitro, they were malignant in vivo, forming vascularized tumors that led to significant morbidity and mortality. To determine the presence of KSHV in the EGFP+ spindle cells of mECK36 tumors, we carried out immunohistochemical determination of KSHV LANA expression. Figures 4B and 4C show that LANA+ cells comprise 30%–50% of mECK36 tumors, which is also reminiscent of KS lesions (Dupin et al., 1999). To further characterize the phenotype of the KSHV-harboring cells in tumors and the status of their KSHV infection, we costained for KSHV LANA, podoplanin, and K8.1. All EGFP+ cells coexpressed LANA and podoplanin (Figure 4B). Confocal images at different Z planes revealed that up to 90% of nuclei were LANA+ and displayed the punctuated pattern indicative of episomal infection (Figure 4D). More than 20% of the tumor cells were also K8.1+ (Figure 4E). To determine changes in the status of KSHV infection in mECK36 due to in vivo growth conditions, we compared the KSHV transcription profiles from three different tumors and from mECK36 in culture (Figure 4F) normalized for LANA in order to include only KSHV-harboring cells (Dittmer, 2003). Compared to cultured mECK36, the tumors showed a 15.6-fold increased expression of lytic genes versus a 1.1-fold increase of latent genes. Since the average variation among the three tumors was only 2.13-fold (CV: 1.93.2.33, n = 91), the increase in lytic mRNA levels must represent a biological response of the viral genome to in vivo growth conditions, rather than a variation introduced by intertumor variation. Despite increased lytic transcription, mECK36 did not show increased viral genome replication, evidenced by the lack of variations in the KSHV viral load and the absence of KSHV virions in the tumors (data not shown). These data indicate that, similar to mECK36 in culture, mECK36 tumors express latent and lytic genes, consistent with an abortive lytic infection, but display increased expression of KSHV lytic genes.

mECK36 Tumors Express KS and Angiogenic Markers

To further determine if the phenotypic markers of the mECK36 sarcomas corresponded to those typically found in human KS lesions, we immunostained for CD31/PECAM (pan-EC marker), VEGF-R2 (EPCs, angiogenically active vessels, KS), and CD34 (EPC, microvascular endothelium, and KS) (Boshoff and Weiss, 2002; Brown et al., 1996; Rafii and Lyden, 2003). The presentation of these markers (Figure 5A) corresponded to a highly vascularized tumor (CD31+ vessels) bearing some VEGF-R2+ vessels as well as VEGF-R2+ and CD34+ cells. To assess the

expression of VEGF receptors in EGFP+ cells, we used immunofluorescence and cytofluorometry analysis for the VEGF-R1 (ECs, proangiogenic hematopoietic cells), VEGF-R2, and VEGF-R3 (lymphatic endothelium and KS) (Hong et al., 2004; Rafii and Lyden, 2003; Wang et al., 2004). A significant percentage of EGFP+ cells displayed the KS and angiogenic markers VEGF-R1, VEGF-R2, and VEGF-R3 (Figure 5A). Cytofluorometric determinations of a representative tumor also showed that EGFP+ cells, which comprised 42% of the tumor, were 60%, 45%, and 40% VEGF-R1+, VEGF-R2+, and VEGF-R3+, respectively (Figures 5D and 5E), compared to 1.5%, 2.0%, and 4.0% of EGFP− cells, comprised by endothelial and stromal cells from the tumor (Figure 5E). To assess the possible upregulation of this angiogenic phenotype in vivo, mRNA levels of VEGF and Angiopoietin family ligands and receptors in mECK36 grown in culture and from nude mice tumors were quantified by real-time RT-PCR. Most of the angiogenic mediators that were upregulated by KSHVBac36 transfection were further upregulated in mECK36 tumors (Figures 2D and 5F). These results indicate that KSHV infection synergizes with in vivo growth conditions to induce the expression of an angiogenic phenotype reminiscent of KS.

mECK36 Mouse Spindle Cell Sarcomas Display KSHV and Host Transcription Profiles Reminiscent of Kaposi's Sarcoma

To gain a perspective of how closely mECK36 KS-like sarcomas resemble primary KS lesions from the standpoint of KSHV expression, we compared the pattern of KSHV transcription in mECK36 sarcomas and in biopsies from KS lesions. By merging data reported here with data from our previous study (Dittmer, 2003), we found that the three mECK36 tumors grouped together, indicating the high reproducibility of the mouse sarcomas (Figure 6A). Six of the primary KS lesions clustered closer to the mECK36 mouse tumors than the five other KS lesions, which, in turn, clustered with cultured mECK36. These results indicate that the pattern of KSHV gene expression obtained in mECK36 cultures and tumors can be considered representative of subpopulations defined by different degrees of lytic gene expression that are found among KS human tumors.

Molecular signatures are a useful way of evaluating the phenotypic identity of tumors (Klein et al., 2001). The KS signature was recently established by identifying 1256 KS genes (1482 probes) that differentiate KS and skin sample groups (Wang et al., 2004). This group of differentially expressed genes is thought to determine key phenotypic differences defining KS, and thus they are primary to the biology of KS tumors. To evaluate the extent to which our mouse model mimics the KS signature, we first determined the transcriptional profile of mECK36 tumors by using genomic arrays, and we identified which genes of the human KS signature were able to differentiate mECK36 tumors and mouse skin ($q < 0.05$) (Figure 6B), defining the mouse KS-like signature. Then, we compared the human and mouse KS-like signature and found that 81% of the transcripts, including many key genes for KS pathophysiology, were equally up- or downregulated in human KS and mouse mECK36 tumors compared to skin (Figure 6B). Using mEC-V, mECK36, and mECK36 tumor microarray data to determine the degree of contribution to the KS-like signature indicates that the major contribution to the signature—close to 50%—was by mECK36 tumors (Figure 6C). In agreement with this microarray analysis, real-time qRT-PCR comparison of angiogenesis-mediating gene expression in mECK36 tumors, cultured mECK36, and mEC-V (Figure 6D) shows that most of the angiogenic gene upregulation takes place when mECK36 grow in vivo to form tumors. Taken together, these results show that KSHV is sufficient to confer to infected cells in vivo angiogenic, tumorigenic, and phenotypic characteristics of KS.

mECK36 Belong to the Endothelial Cell Lineage

The KS-like phenotype of mECK36 tumors suggests that Bac36 was originally transfected to a cell lineage closely related to the one that leads to KS in human KSHV infection. More accurate determination of the cell lineage that gave rise to mECK36 could point to a KS spindle cell progenitor. Genomic profiling provides a useful way to trace the cell of origin of transformed cells (Klein et al., 2001). To further identify the progenitor(s) cell type that was targeted by KSHVBac36 transfection among the heterogeneous mEC population, we used the genome-wide transcription profile of mEC-V and mECK36 and clustered it to several mouse cell types that can be present in the mECs, including ECs, endothelial progenitors, and hematopoietic progenitors. As shown in Figure S1 (see the Supplemental Data available with this article online), mEC-V and mECK36 cluster in between endothelial progenitors and mature vascular ECs, further supporting the endothelial-lineage origin of mECK36.

mECK36 Tumorigenicity Is Reversible and Strictly KSHV Dependent

mECK36 cultures and tumors are a valuable tool for defining the function of KSHV pathogenic genes and their relationship with host responses and KSHV biology. The phenotypic differences between mEC-V and mECK36 is thought to be a consequence of KSHVBac36 transfection with concomitant KSHV gene expression in normal cell progenitors, and it is consistent with the proposed KSHV-induced phenotype in KS. However, to demonstrate a link between KSHV and mECK36 tumorigenesis, it is necessary to show the dependency between KSHV gene expression and the KS-like phenotype. This is because mECK36 could have accumulated host gene oncogenic alterations that may contribute to the malignant phenotype independently of KSHV. This can be demonstrated by showing that mECK36 that have lost the KSHV genome lose the ability to form KS-like tumors. It was previously shown that episomal KSHV is lost from cells in culture unless it is maintained by antibiotic selection (Grundhoff and Ganem, 2004). Episomally infected mECK36 are routinely selected in Hyg-containing media for the maintenance of the Hyg^r KSHVBac36. To test whether mECK36 cultured

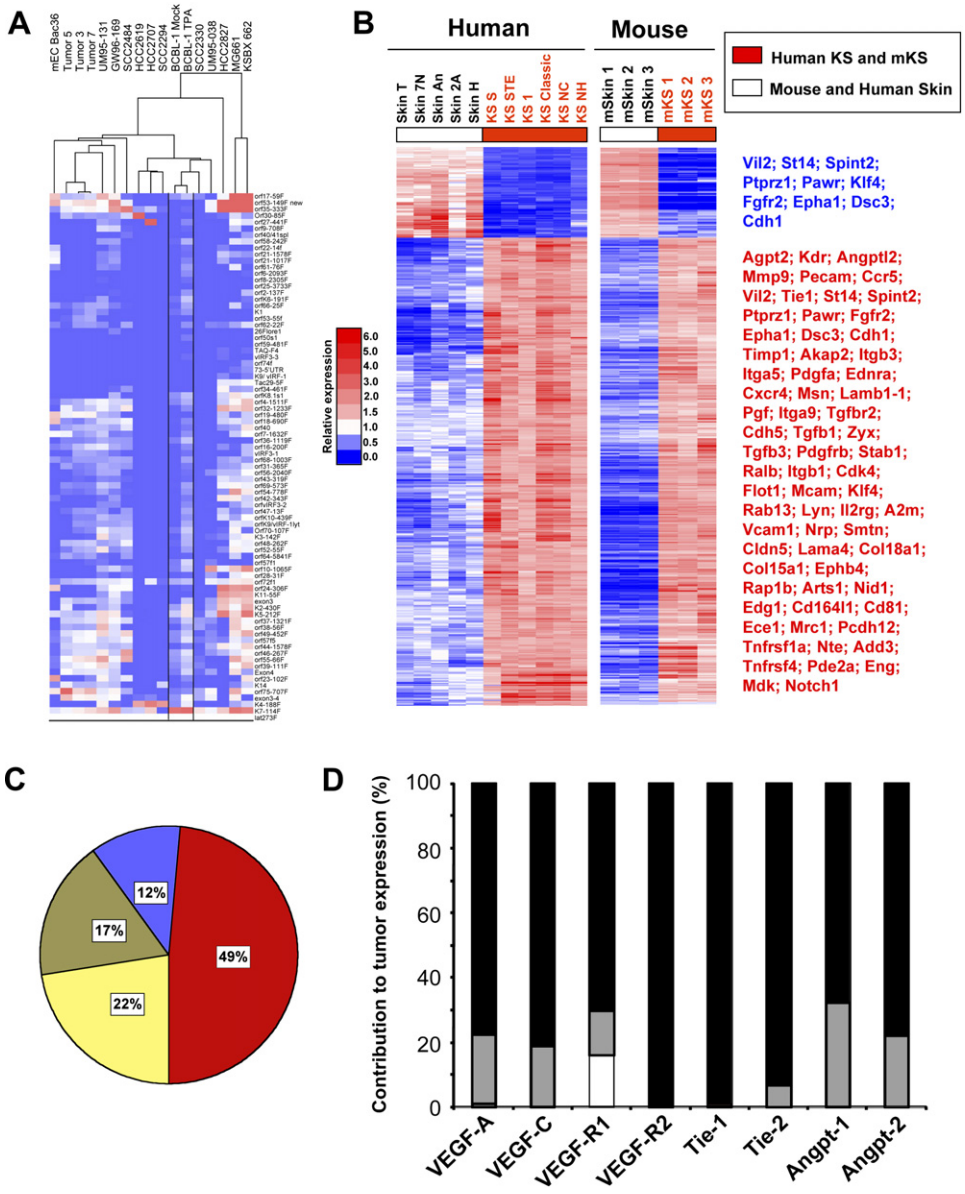

Figure 6. Viral and Host Global Gene Expression of mECK36 Tumors Resembles KS

(A) Clustering of primary KS with mEC-Bac36 tumors. The heatmap represents real-time qRT-PCR results. Tumors 5, 3, and 7 are three mECK36 spindle cell sarcomas. BCBL Mock and TPA are BCBL-1 uninduced and induced with TPA, respectively.

(B) Heatmap representation of 562 genes ($q < 0.05$) of the human KS signature that behave as the mECK36 tumor signature (equally up- or down-regulated). A total of 723 genes from the human KS signature were orthologs to mouse genes present in the mouse affymetrix array. Among these, 691 genes were able to differentiate mECK36 spindle cell sarcomas and mouse skin ($q < 0.05$) for at least a 2-fold difference. A total of 471 genes (68%) and 91 genes (13%) were upregulated (red) and downregulated (blue), respectively, in both mECK36 tumors and human KS. Selected down-regulated genes are shown in blue, and upregulated genes are shown in red. The full list of genes is available in Table S1.

(C) Distribution of the mouse KS signature. Blue, genes shared between mECK36 tumors and mEC-V; yellow, genes shared between mECK36 tumors and mECK36 in culture; Olive, genes shared by mEC-V, mECK36 in culture, and tumors; Red, mECK36 tumors only. Gene intensity from the mouse KS signature was set to 100%, and the percentage of genes that contribute to the mouse KS signature was calculated by using a 10% difference in intensity between the different samples and tumors (GeneSpring 7 package).

(D) Angiogenic gene expression in mEC-V and in mECK36 relative to that in mECK36 tumors. mRNA levels were determined by real-time qRT-PCR. mRNA levels in tumors were set at 100% (closed bar). Overlapped are bars representing relative mRNA levels in mECK36 in culture (gray bars) and in mEC-V (open bars) (mean of triplicates ± SEM). Relative levels were calculated as a (1/fold increase in tumors) × 100.

in the absence of antibiotic selection lose the KSHVBac36 episome, cultured mECK36 and mECK36 explanted from tumors were cultured in the presence or the absence of Hyg. We found that both mECK36 and explanted mECK36 tumor cells lost the BacKSHV episome after 4 weeks of culture without Hyg, as evidenced by loss of

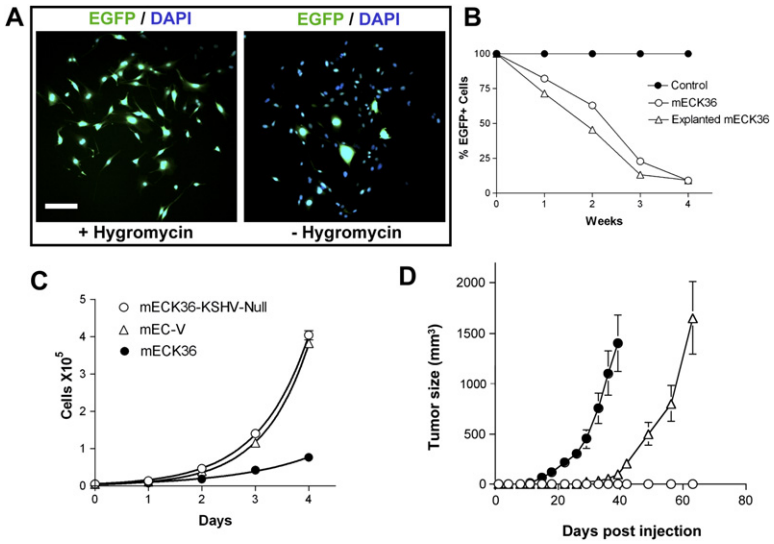

Figure 7. mECK36 Tumorigenicity Is Reversible and Strictly KSHV Dependent

(A) Many cells in colonies that originated from a single EGFP+ mECK36 became EGFP− when grown in the absence of Hyg.

(B) EGFP levels of cultured and explanted mECK36 grown with or without Hyg determined by flow cytometry. mECK36 grown in Hyg media were used as controls and were set at 100% for every passage.

(C) In vitro growth rate of mECK36, mEC-V, and KSHV null mECK36. Doubling times were 22, 14, and 15 hr, respectively.

(D) Tumor formation of KSHV null mECK36 (open circles), mECK36 (closed circles), and a 1:1000 ratio of mECK36:KSHV null mECK36 (open triangles). Data indicate mean tumor size ± SEM (n = 5). The scale bar is 100 μM.

EGFP fluorescence (Figures 7A and 7B). To demonstrate that this effect was actual episome loss and not outgrowth by EGFP− cells, we carried out a colony formation assay in plastic, in which we monitored colonies originated from a single EGFP+ mECK36. EGFP+ mECK36 single-cell clones grown without Hyg lost their episomes and became EGFP− as they divided (Figure 7A, peripheral cells). These results have several implications: (1) the rapid loss of the episome in vitro suggests that mECK36 that lost the KSHV episome had a selective advantage over KSHV+ cells; (2) the generation of nonfluorescent and Hyg-sensitive cultured and tumor-explanted cells indicates that the KSHVBac36 is only present as an episome and is not integrated in the host genome; (3) KSHV provides an in vivo selective advantage equivalent to Hyg in vitro since mECK36 explanted from the tumor lose the episome and tumors are grown in the absence of Hyg. We compared KSHV+ mECK36 with mECK36 that have lost the KSHV episome (KSHV null mECK36). While KSHV null mECK36 or mEC-V have a higher growth rate in vitro than mECK36 (Figure 7C), KSHV null mECK36 completely lost tumorigenicity in mice. Moreover, a mixture of 1:1000 of mECK36:KSHV null mECK36 have delayed tumor growth in mice, which leads to the formation of tumors similar in size to those induced by mECK36 alone (Figure 7D). Analysis of these tumors shows up to 30% EGFP+/KSHV LANA+ mECK36 (data not shown). These results demonstrate that KSHV provides a selective advantage in vivo, but not in vitro, and that mECK36 tumorigenesis is strictly dependent on KSHV since it can be reversed by loss of the KSHV episome.

Role of KSHV Gene Expression and the Angiogenic Oncogene vGPCR in Sarcomagenesis

KSHV dependency suggests that mECK36 tumors are a biologically sensitive model in which we can study the role of KSHV genes in KS pathogenesis. A mechanistic explanation for mECK36 tumorigenesis is that KSHV genes upregulated during in vivo growth induce mECK36's malignancy by activating cell proliferation, cell survival, or angiogenic gene expression (Figures 5F and 6D). We found that the KSHV genes most upregulated when mECK36 form tumors encode for proteins that have been implicated in inhibition of p53-induced apoptosis (vIRF-1) (Nakamura et al., 2001), JNK signaling (ORF36) (Hamza et al., 2004), and angiogenesis activation (vGPCR) (Figure 8A). Since vGPCR has been shown to induce a KS-like angiogenic phenotype by activating VEGF expression (Bais et al., 1998, 2003; Grisotto et al., 2006; Guo et al., 2003; Montaner et al., 2003, 2006; Yang et al., 2000), we speculated on the possibility that vGPCR upregulation leading to VEGF secretion was causally linked to mECK36 tumorigenesis. As a proof of principle for the use of mECK36 in genetic studies of KSHV pathogenesis, we silenced vGPCR by RNA interference (RNAi) by using a vGPCR short hairpin RNA (shRNA) (Figure 8B) and assessed the impact on mECK36 angiogenesis and tumorigenicity. To determine whether the RNAi suppression affected other KSHV pathogenic genes, we performed real-time RT PCR array analysis on shRNA or control transfected mECK36 (Figure 8C). While the level for most of the KSHV mRNAs remained unchanged, as evidenced by the clustering of data points on the 45° line ($m = 1.00$, $r^2 = 0.95$, $n = 93$), the vGPCR message was reduced 117-fold. We also observed a reduction of the mRNAs for ORFs 7, 25, 26, and 27. The significant decrease on the mRNA levels of these ORFs strongly suggests that cellular signaling pathways activated by vGPCR might, in turn, feed back on the virus to control the expression of these KSHV genes. shRNA-mediated silencing of vGPCR in mECK36 blocked their ability to secrete VEGF and significantly reduced the ability of the mECK36 to induce microvessel formation in skin (Figure 8D) ($p < 0.05$). Although both vGPCR shRNA and control shRNA-transfected mECK36 grew at a very similar rate in culture (not shown), vGPCR shRNA mECK36 tumors showed delay and

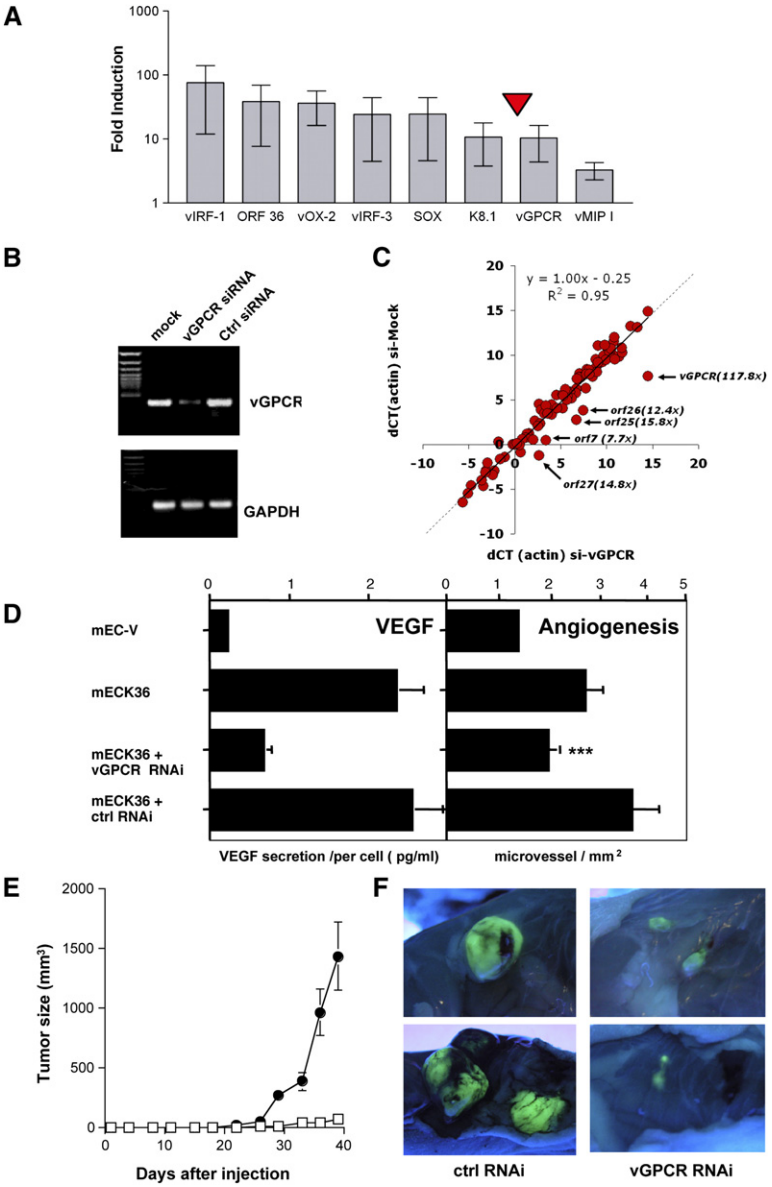

Figure 8. RNAi-Mediated Suppression of KSHV vGPCR in mECK36 Blocks Angiogenicity and Tumorigenesis

(A) Increase in mRNA level of KSHV genes in mECK36 tumors compared to cultured mECK36 determined by real-time qRT-PCR. Mean values (±SD) from three tumor samples were plotted.

(B) RT-PCR analysis of vGPCR and GAPDH for mECK36 transfected with control shRNA and vGPCR shRNA vector.

(C) Log2 scale plot (dCT) of the actin-normalized KSHV mRNA levels of mECK36 transfected with control shRNA (horizontal) or vGPCR shRNA (vertical). The arrows indicate transcripts that are specifically downregulated, and the annotation shows the identity and fold downregulation.

(D) Left panel: levels of VEGF secretion for mECK36 transfected with either control shRNA or vGPCR shRNA vector measured by ELISA. Bars indicate mean of duplicate measures ± range. Right panel: angiogenesis in skin for mEC-V, mECK36, mECK36 transfected with either control shRNA or vGPCR shRNA vector. The bar graphs show the mean microvessel density (vessels/mm^2) ± SEM. Total n (both flanks) = 10. ***Significant differences between vGPCR RNAi and control RNAi groups ($p < 0.05$) (n = 10).

(E) Tumor formation of mECK36 transfected with control shRNA (closed circles) or with vGPCR shRNA vector (open squares). Data indicate mean tumor size ± SEM (n = 10).

(F) Tumor appearance after dissection and lighting by using a long-wave UV lamp for mECK36 transfected with control shRNA or with vGPCR shRNA vector.

inhibition in tumor formation (Figure 8E), which is consistent with a reduction in angiogenicity (Folkman, 1995). These results show that activation of angiogenesis by KSHV vGPCR is causally implicated in mECK36 tumorigenesis and demonstrate that mECK36 can be genetically manipulated to study KSHV pathobiology.

DISCUSSION

A normal progenitor cell derivative containing the entire KSHV genome allowed for the reproduction of the tumorigenic and angiogenic characteristics of an infected KS spindle cell and led to the generation of a cell and animal model of KSHV-induced KS. This model not only illustrates several features that makes it useful for biological and preclinical studies, but it also challenges our current thinking on key issues of KSHV biology and KS pathogenesis.

We found that the KSHV genome is angiogenic and tumorigenic in endothelial-lineage cells of adherent bone marrow cell preparations. These findings suggest that an endothelial-lineage cell type is a natural target of KSHV infection and a progenitor of tumorigenic KS spindle cells. It should be added that although our approach allows us to "target" putative progenitors in the transfected population and may have been critical for inclusion of the right cell type(s) in the right microenvironment, it does not allow us to unequivocally identify the KSHV targets. Nevertheless, phenotypic marker expression and transcriptome profile clustering results are consistent with the KSHVBac36 being transfected to endothelial-lineage cells that are among the bone marrow adherent-cell population, including ECs and EC progenitors (Rafii and Lyden, 2003).

We showed that the KSHV genome can independently induce the KS phenotype when its genome is expressed

within the context of an appropriate normal cell progenitor and when the KSHV-bearing cells are grown in vivo. mECK36 lead to the growth of subcutaneous tumors or multifocal KS pulmonary lesions consisting of vascular spindle cell sarcomas that expressed angiogenic and KS phenotypic markers such as podoplanin and the VEGF and Angiopoietin receptors and ligands. Moreover, genome-wide transcriptome analysis of mECK36 tumors revealed that 81% of human KS signature genes behaved as mECK36 tumor signature genes and were similarly up- or downregulated in mouse and human tumors. These findings suggest that the KSHV genome encodes the ability to recreate the full KS pathophysiology, including visceral invasiveness and disease localization.

The pattern of KSHV expression in tumors, as evidenced by RT-PCR array analysis and immunodetection of K8.1, was consistent with an increase in lytic transcripts. Although it was reported that most spindle cells in KS lesions are latently infected (Staskus et al., 1997), we found that a subpopulation of KS lesions (Dittmer, 2003) exhibits a pattern of KSHV expression similar to mECK36 spindle sarcomas. Thus, the KSHV expression profile of mECK36 in tumors can be biologically relevant. In future studies, it will be of importance to establish possible correlations between the mECK36-like KSHV expression profile and KS clinical presentation. Interestingly enough, the mECK36 pattern of KSHV gene expression was not accompanied by virus production, indicating that mECK36 were in an abortive lytic replication state. Others have shown that in permissive human cells KSHVBac36 transfection leads to virion production (Zhou et al., 2002). In contrast, both in vitro and in vivo grown mECK36 showed an absence of viral replication. Since transcriptome analysis shows that the viral genome is intact, it is unlikely that the defects in viral replication were due to Bac36 alterations. Instead, viral replication and maturation events are most likely being blocked. A recent report (Parsons et al., 2006) points to productive KSHV infection in SCID/NOD mice upon injection of KSHV virions, suggesting that the use of KSHVBac36 transfection may relate to the abortive lytic status of mECK36. Interestingly, KS lesions contain lytic replication-defective KSHV genomes that may play a role in KS tumorigenesis (Deng et al., 2004). Thus, the replication-defective infection achieved by Bac36 transfection may be relevant to actual occurrences of the disease and might have been critical to capture a KSHV-induced KS phenotype.

We found that KSHV episome loss led to loss of tumorigenicity. This indicates that the mECK36 tumorigenic phenotype is strictly dependent on KSHV and reversible, since mECK36 reverted to a nontumorigenic phenotype upon KSHV loss in vitro. This resembles explanted KS spindle cells that lose KSHV in culture and become nontumorigenic (Aluigi et al., 1996; Dictor et al., 1996; Ganem, 2006). It also suggests that KSHV-induced oncogenesis, at least in its initial stages, does not lead to the accumulation of additional oncogenic hits that could contribute to a malignant phenotype independent of KSHV. This also resembles human KS lesions in which cellular oncogenic alterations such as p53 and ras mutations, or Bcl-2 overexpression together with increased clonality, tend to be found only in advanced KS (Gill et al., 1998; Nicolaides et al., 1994; Pillay et al., 1999; Rabkin et al., 1997). It can also be concluded that the maintenance of the KSHV episome during tumor formation—which is carried out in the absence of Hyg—indicates that KSHV does provide a selective advantage for in vivo growth that leads to tumorigenesis. This selective advantage of KSHV+ versus non-infected cells provides an alternative explanation to reinfection (Grundhoff and Ganem, 2004) for maintenance of the KSHV episome in infected spindle cells in KS lesions.

KSHVBac36-mediated tumorigenesis correlated with the upregulation of several KSHV lytic transcripts and the induction of a KS-like angiogenic phenotype upon implantation into nude mice. This further supports the notion, evidenced by recent publications, that in KS as well as in PEL (An et al., 2006; Staudt et al., 2004) the host microenvironment influences KSHV gene expression. However, the regulatory effects are indeed reciprocal. We found that KSHV together with in vivo growth conditions trigger in the infected cell the expression of genes related to angiogenesis and malignancy, which provides a selective advantage and leads to tumor formation. We found that mECK36 grown in vitro did not display signs of cell transformation. When subjected to in vivo growth conditions, however, the same cells induced angiogenic spindle cell sarcomas with upregulation of key angiogenic markers (Figures 5F and 6D). In concordance, analysis of the mouse KS-like signature of mECK36 tumors showed that almost 50% of it derives from genes that were only expressed in mECK36 tumors. The concomitant upregulation of KSHV lytic genes in vivo and the induction of an angiogenic phenotype in KS-like lesions pointed to a series of potentially pathogenic KSHV genes as critical determinants of KS-like tumorigenesis. We selectively inhibited one of these genes to prove its involvement in mECK36 tumorigenesis and to test the suitability of our model for genetic analysis of KSHV pathogenic function. siRNA-mediated suppression of the early lytic angiogenic oncogene vGPCR (Bais et al., 1998, 2003; Yang et al., 2000) blocked VEGF secretion and tumorigenesis, leading to significant retardation in tumor growth. It is unlikely that siRNA was also targeting the expression of ORF K14, which is coexpressed with vGPCR in bicistronic messages (Kirshner et al., 1999), as ORF K14 mRNA levels were not affected by the vGPCR shRNA (Figure 8C). These results with vGPCR silencing were verified by preliminary studies with vGPCR null Bac36 mutants (L.E.C. and E.A.M., unpublished data). Our results confirm single-gene experiments with vGPCR (Bais et al., 1998, 2003; Grisotto et al., 2006; Guo et al., 2003; Montaner et al., 2003, 2006; Yang et al., 2000), indicating that it plays a nonredundant role in angiogenesis and tumorigenesis within the context of full KSHV genome expression, and they further support the notion that this KSHV gene is a good therapeutic target. Our results with vGPCR suppression show that our model is sensitive to genetic manipulation

and can be used to analyze the contribution of other KSHV genes in tumorigenesis. Furthermore, they point to a mECK36 in vivo malignant phenotype as a consequence of upregulation of KSHV genes, such as vGPCR, that provide a selective advantage to the cell—in this case angiogenicity—leading to positive selection of the KSHV episome and KS-like tumor formation.

The suitability of mECK36 for genetic studies of KS pathogenesis could help to reveal the role of both KSHV and host genes implicated in the KS phenotype. A recent report showed that long-term latent KSHV infection of immortalized human ECs leads to the outgrowth of transformed and tumorigenic clones (An et al., 2006). However, the use of hTERT-immortalized cells as substrates, and the sporadic occurrence of the in vitro-transformed outgrowths point to the accumulation of oncogenic alterations in the host genome; thus, making it difficult to strictly link the malignant phenotype to specific KSHV genes. In our case, the fact that Bac36 transfection of mECs leads to a nonproductive infection also imposes limitations to the mECK36 model, in particular for studying viral entry and viral replication. However, several key characteristics make the mECK36 model appropriate for genetic studies of pathobiology and experimental therapeutics: (1) the progenitor target population(s) is normal mouse bone marrow cells, making it possible to use available knockout (KO) or conditional KO mice to generate different Bac36-transfected cells that could be used to identify genetic determinants of KS pathogenesis; (2) the KSHV dependence of the KS phenotype makes the mECK36 system highly sensitive for studies of KSHV genes critical for tumor growth and makes it suitable for testing therapeutic strategies targeting KSHV pathogenic genes or host angiogenic machinery; (3) the mECK36 population expresses the full KSHV genetic complement, allowing for manipulation of latent and lytic KSHV genes by using Bac or siRNA in functional studies; (4) mECK36 viral expression was stable through multiple passages (D.P.D. and E.A.M., unpublished data) and had reproducible in vivo pathogenic phenotypes.

In summary, our results show that the mEC Bac36 system and the mECK36 KSHV-harboring spindle sarcomas are good phenotypic, physiologic, molecular, and viral surrogates of human KS that could unlock research avenues for KSHV pathobiology. They define mECK36 as a biologically sensitive cell and animal model of viral KS suitable for analyzing the role of KSHV and host cell genes in KS pathogenesis, as well as for preclinical testing of anti-KS drugs.

EXPERIMENTAL PROCEDURES

Vectors and Constructs

The empty vector pMHGP and the vector containing the insert with the genome of KSHV in Bacterial Artificial Chromosome (KSHVBac36) were obtained as described previously (Zhou et al., 2002). The empty vector pSilencer 2.1-U6 neo and the shRNA control vector were obtained from Ambion (Austin, TX). To obtain the hairpin sequences that silence the expression of vGPCR, we selected candidate sequences for low homology to mouse transcripts by BLAST search. The selected sequences were 5′-GATCCCATGTTCTTGGAAATGG ATTTTCAAGAGAAATCCATTTCCAAGAACATTTTTTTGGAAA-3′ and 5′-AGCTTTTCCAAAAAATGTTCTTGGAAATGGATTTCTCTTGAAAAT CCATTTCCAAGAACATGG-3′, which created vGPCR shRNA hairpin loops with BamHI- and HindIII-specific sticky ends to be cloned in pSilencer 2.1-U6 neo. All of the transfections were performed by using Lipofectamine 2000 (Invitrogen, Carlsbad, CA). Cells transfected with KSHVBac36 or vector were selected with Hyg-B. For pSilencer 2.1-U6 neo vGPCR or control vector, cells were double selected with Hyg-B and G418 (Sigma, Saint Louis, Missouri).

Cells

mECs were obtained from Balb/C An Ncr-nu mice (NCI, Bethesda, MD) bone marrow. Mice femurs were flushed twice with PBS, and the eluates were incubated in DMEM media plus 30% FBS (Gemini Bioproducts, Calabasas, CA), 0.2 mg/ml Endothelial Growth Factor (EGF) (Sigma, Saint Louis, MO), 0.2 mg/ml Endothelial Cell Growth Factor Supplement (ECGS) (Sigma, Saint Louis, Missouri), 1.2 mg/1 heparin (Sigma, Saint Louis, MO), insulin transferrin selenium (Invitrogen, Carlsbad, CA), 1% penicillin-streptomycin (Invitrogen, Carlsbad, CA), and BME vitamin (VWR Scientific, Rochester, NY). NIH 3T3 cells were purchased from American Type Culture Collection. RasV12-transformed NIH 3T3 cells were obtained as described (Bais et al., 1998).

Animals

Eight-week-old male Balb/C An Ncr-nu mice (NCI, Bethesda, MD) were used for angiogenesis assays and subcutaneous tumors. Twelve-week-old male SCID/NOD ICRSC-M mice (Taconic, Germantown, NY) were used for intravenous injection of cells. Mice were kept under sterile conditions and were used under protocols approved by the Institutional Animal Care and Use Committee.

Angiogenesis Assay

A total of 3×10^5 cells (two inoculation sites per mouse) were inoculated intradermally in Balb/C nude mice. Trypan blue (20%) was used to assess cell viability and mark the inoculation site. Mice (five per group) were sacrificed 5 days later, and the surface area of the injection site was exposed by dissection and was photographed with a stereoscopic microscope (Nikon Corporation, Tokyo, Japan). To assess microvessel density, the whole surface area of the injection site was examined for morphometric analysis by following Auerbach's criteria (Auerbach et al., 2000). To this extent, each photograph slide was projected in a grid corresponding to 1^2 mm, and the total number of individual blood microvessels on all grids was counted in a blinded labeled fashion. The blood density was defined as the number of vessels per grid (D = total number of vessels/total number of grids counted).

Mouse Tumor Growth Assays

Mice (n = 7) were inoculated subcutaneously with cells (3×10^5 per mouse). Tumor growth was followed by caliper measurements of volume until the date of sacrifice. mECK36 tumors were allowed to grow until they reached a volume of $\sim$2 cm^3. SCID/NOD mice (n = 5) were irradiated (350 rad) and, after 3 hr, were inoculated intravenously (IV) in the tail vein (2×10^6 cells per mouse). Mice were followed for 3 months until symptoms of distress such as dyspnea and pain, at which point they were sacrificed and complete necropsies were performed.

Other Experimental Procedures

For details on immunofluorescence, immunohistochemistry, real-time qRT-PCR, VEGF Elisa, flow cytometry of tumor, microarray procedures and analysis, and statistical methods, see Supplemental Data.

Supplemental Data

The Supplemental Data include Supplemental Experimental Procedures, one supplemental figure, and one supplemental table and are available at http://www.cancercell.org/cgi/content/full/11/3/245/DC1/.

ACKNOWLEDGMENTS

This paper is dedicated to Philip Juan Browning (1953-2004), who made the initial observations on the existence of circulating hematopoietic KS progenitors. We would like to thank Rafael Tejada and David K. Jin for their help and support. We are grateful to Dr. Don Ganem for his thoughtful critiques of earlier versions of this work and Dr. Ethel Cesarman for her helpful comments and her continuous support of our work. We are thankful to Dr. Beata Frydel and Brigitte Shaw from the Imaging and Molecular Core Facility (DRI, University of Miami). We thank Dr. Adam Asch, Dr. Roger Pierce, Anne Marie Valadere, and Heidi Kiger for comments on the manuscript. We are indebted to Aileen Chen for her excellent editing job. We are thankful to Drs. David Salomon and Sunil Kurian for facilitating their array data sets. This work was supported by National Institutes of Health grants CA 075918 to E.A.M, CA096512 to S.-J.G., and CA110136 and CA109232 to D.P.D; by a grant from the Dorothy Rodbell Cohen Foundation for Sarcoma Research to E.A.M.; and by the Viral Oncology Program of the Sylvester Comprehensive Cancer Center (E.A.M.).

Received: June 7, 2006
Revised: October 13, 2006
Accepted: January 4, 2007
Published: March 12, 2007

REFERENCES

Aluigi, M.G., Albini, A., Carlone, S., Repetto, L., De Marchi, R., Icardi, A., Moro, M., Noonan, D., and Benelli, R. (1996). KSHV sequences in biopsies and cultured spindle cells of epidemic, iatrogenic and Mediterranean forms of Kaposi's sarcoma. Res. Virol. *147*, 267–275.

An, F.Q., Folarin, H.M., Compitello, N., Roth, J., Gerson, S.L., McCrae, K.R., Fakhari, F.D., Dittmer, D.P., and Renne, R. (2006). Long-term-infected telomerase-immortalized endothelial cells: a model for Kaposi's sarcoma-associated herpesvirus latency in vitro and in vivo. J. Virol. *80*, 4833–4846.

Aoki, Y., Jaffe, E.S., Chang, Y., Jones, K., Teruya-Feldstein, J., Moore, P.S., and Tosato, G. (1999). Angiogenesis and hematopoiesis induced by Kaposi's sarcoma-associated herpesvirus-encoded interleukin-6. Blood *93*, 4034–4043.

Auerbach, R., Akhtar, N., Lewis, R.L., and Shinners, B.L. (2000). Angiogenesis assays: problems and pitfalls. Cancer Metastasis Rev. *19*, 167–172.

Bais, C., Santomasso, B., Coso, O., Arvanitakis, L., Raaka, E.G., Gutkind, J.S., Asch, A.S., Cesarman, E., Gershengorn, M.C., and Mesri, E.A. (1998). G-protein-coupled receptor of Kaposi's sarcoma-associated herpesvirus is a viral oncogene and angiogenesis activator. Nature *391*, 86–89.

Bais, C., Van Geelen, A., Eroles, P., Mutlu, A., Chiozzini, C., Dias, S., Silverstein, R., Rafii, S., and Mesri, E.A. (2003). Kaposi's sarcoma associated herpesvirus G protein coupled receptor immortalizes human endothelial cell by activation of the VEGF receptor-2/KDR. Cancer Cell *3*, 131–143.

Ballestas, M.E., Chatis, P.A., and Kaye, K.M. (1999). Efficient persistence of extrachromosomal KSHV DNA mediated by latency-associated nuclear antigen. Science *284*, 641–644.

Barozzi, P., Luppi, M., Facchetti, F., Mecucci, C., Alu, M., Sarid, R., Rasini, V., Ravazzini, L., Rossi, E., Festa, S., et al. (2003). Post-transplant Kaposi sarcoma originates from the seeding of donor-derived progenitors. Nat. Med. *9*, 554–561.

Boshoff, C., and Weiss, R.A. (1998). Kaposi's sarcoma-associated herpesvirus. Adv. Cancer Res. *75*, 57–86.

Boshoff, C., and Weiss, R. (2002). AIDS-related malignancies. Nat. Rev. Cancer *2*, 373–382.

Boshoff, C., Endo, Y., Collins, P.D., Takeuchi, Y., Reeves, J.D., Schweickart, V.L., Siani, M.A., Sasaki, T., Williams, T.J., Gray, P.W., et al. (1997). Angiogenic and HIV-inhibitory functions of KSHV-encoded chemokines. Science *278*, 290–294.

Brown, L.F., Tognazzi, K., Dvorak, H.F., and Harrist, T.J. (1996). Strong expression of kinase insert domain-containing receptor, a vascular permeability factor/vascular endothelial growth factor receptor in AIDS-associated Kaposi's sarcoma and cutaneous angiosarcoma. Am. J. Pathol. *148*, 1065–1074.

Browning, P.J., Sechler, J.M.G., Kaplan, M., Washington, R.H., Gendelman, R., Yarchoan, R., Ensoli, B., and Gallo, R.C. (1994). Identification and culture of Kaposi's sarcoma-like spindle cells from the peripheral blood of human immunodeficiency virus-1 individualas and normal controls. Blood *84*, 2711–2720.

Cesarman, E., Chang, Y., Moore, P.S., Said, J.W., and Knowles, D.M. (1995). Kaposi's sarcoma-associated herpes virus-like DNA sequences are present in AIDS-related body cavity B-cell lymphomas. N. Engl. J. Med. *332*, 1186–1191.

Chang, Y., Cesarman, E., Pessin, M.S., Lee, F., Culpepper, J., Knowles, D., and Moore, P. (1994). Identification of herpesvirus-like DNA sequences in AIDS-associated Kaposis's sarcoma. Science *266*, 1865–1869.

Ciufo, D.M., Cannon, J.S., Poole, L.J., Wu, F.Y., Murray, P., Ambinder, R.F., and Hayward, G.S. (2001). Spindle cell conversion by Kaposi's sarcoma-associated herpesvirus: formation of colonies and plaques with mixed lytic and latent gene expression in infected primary dermal microvascular endothelial cell cultures. J. Virol. *75*, 5614–5626.

Deng, J.H., Zhang, Y.J., Wang, X.P., and Gao, S.J. (2004). Lytic replication-defective Kaposi's sarcoma-associated herpesvirus: potential role in infection and malignant transformation. J. Virol. *78*, 11108–11120.

Dictor, M., Rambech, E., Way, D., Witte, M., and Bendsoe, N. (1996). Human herpesvirus 8 (Kaposi's sarcoma-associated herpesvirus) DNA in Kaposi's sarcoma lesions, AIDS Kaposi's sarcoma cell lines, endothelial Kaposi's sarcoma simulators, and the skin of immunosuppressed patients. Am. J. Pathol. *148*, 2009–2016.

Dittmer, D.P. (2003). Transcription profile of Kaposi's sarcoma-associated herpesvirus in primary Kaposi's sarcoma lesions as determined by real-time PCR arrays. Cancer Res. *63*, 2010–2015.

Dupin, N., Fisher, C., Kellam, P., Ariad, S., Tulliez, M., Franck, N., van Marck, E., Salmon, D., Gorin, I., Escande, J.P., et al. (1999). Distribution of human herpesvirus-8 latently infected cells in Kaposi's sarcoma, multicentric Castleman's disease, and primary effusion lymphoma. Proc. Natl. Acad. Sci. USA *96*, 4546–4551.

Fakhari, F.D., and Dittmer, D.P. (2002). Charting latency transcripts in Kaposi's sarcoma-associated herpesvirus by whole-genome real-time quantitative PCR. J. Virol. *76*, 6213–6223.

Flore, O., Rafii, S., Ely, S., O'Leary, J.J., Hyjek, E.M., and Cesarman, E. (1998). Transformation of primary human endothelial cells by Kaposi's sarcoma-associated herpesvirus. Nature *394*, 588–592.

Folkman, J. (1995). Angiogenesis in cancer, vascular, rheumatoid and other disease. Nat. Med. *1*, 27–31.

Gallo, R.C. (1998). The enigmas of Kaposi's sarcoma. Science *282*, 1837–1839.

Ganem, D. (2006). KSHV infection and the pathogenesis of Kaposi's sarcoma. Annu. Rev. Pathol. Mech. Dis. *1*, 273–296.

Gao, S.J., Boshoff, C., Jayachandra, S., Weiss, R.A., Chang, Y., and Moore, P.S. (1997). KSHV ORF K9 (vIRF) is an oncogene which inhibits the interferon signaling pathway. Oncogene *15*, 1979–1985.

Gill, P.S., Tsai, Y.C., Rao, A.P., Spruck, C.H., 3rd, Zheng, T., Harrington, W.A., Jr., Cheung, T., Nathwani, B., and Jones, P.A. (1998). Evidence for multiclonality in multicentric Kaposi's sarcoma. Proc. Natl. Acad. Sci. USA *95*, 8257–8261.

Grisotto, M.G., Garin, A., Martin, A.P., Jensen, K.K., Chan, P., Sealfon, S.C., and Lira, S.A. (2006). The human herpesvirus 8 chemokine

receptor vGPCR triggers autonomous proliferation of endothelial cells. J. Clin. Invest. *116*, 1264–1273.

Grundhoff, A., and Ganem, D. (2004). Inefficient establishment of KSHV latency suggests an additional role for continued lytic replication in Kaposi sarcoma pathogenesis. J. Clin. Invest. *113*, 124–136.

Guo, H.G., Sadowska, M., Reid, W., Tschachler, E., Hayward, G., and Reitz, M. (2003). Kaposi's sarcoma-like tumors in a human herpesvirus 8 ORF74 transgenic mouse. J. Virol. *77*, 2631–2639.

Hamza, M.S., Reyes, R.A., Izumiya, Y., Wisdom, R., Kung, H.J., and Luciw, P.A. (2004). ORF36 protein kinase of Kaposi's sarcoma herpesvirus activates the c-Jun N-terminal kinase signaling pathway. J. Biol. Chem. *279*, 38325–38330.

Hong, Y.K., Foreman, K., Shin, J.W., Hirakawa, S., Curry, C.L., Sage, D.R., Libermann, T., Dezube, B.J., Fingeroth, J.D., and Detmar, M. (2004). Lymphatic reprogramming of blood vascular endothelium by Kaposi sarcoma-associated herpesvirus. Nat. Genet. *36*, 683–685.

Kirshner, J.R., Staskus, K., Haase, A., Lagunoff, M., and Ganem, D. (1999). Expression of the open reading frame 74 (G-protein-coupled receptor) gene of Kaposi's sarcoma (KS)-associated herpesvirus: implications for KS pathogenesis. J. Virol. *73*, 6006–6014.

Klein, U., Tu, Y., Stolovitzky, G.A., Mattioli, M., Cattoretti, G., Husson, H., Freedman, A., Inghirami, G., Cro, L., Baldini, L., et al. (2001). Gene expression profiling of B cell chronic lymphocytic leukemia reveals a homogeneous phenotype related to memory B cells. J. Exp. Med. *194*, 1625–1638.

Knight, J.S., Cotter, M.A., 2nd, and Robertson, E.S. (2001). The latency-associated nuclear antigen of Kaposi's sarcoma-associated herpesvirus transactivates the telomerase reverse transcriptase promoter. J. Biol. Chem. *276*, 22971–22978.

Lagunoff, M., Bechtel, J., Venetsanakos, E., Roy, A.M., Abbey, N., Herndier, B., McMahon, M., and Ganem, D. (2002). De novo infection and serial transmission of Kaposi's sarcoma-associated herpesvirus in cultured endothelial cells. J. Virol. *76*, 2440–2448.

Lee, H., Veazey, R., Williams, K., Li, M., Guo, J., Neipel, F., Fleckenstein, B., Lackner, A., Desrosiers, R.C., and Jung, J.U. (1998). Deregulation of cell growth by the K1 gene of Kaposi's sarcoma-associated herpesvirus. Nat. Med. *4*, 435–440.

Montaner, S., Sodhi, A., Molinolo, A., Bugge, T.H., Sawai, E.T., He, Y., Li, Y., Ray, P.E., and Gutkind, J.S. (2003). Endothelial infection with KSHV genes in vivo reveals that vGPCR initiates Kaposi's sarcomagenesis and can promote the tumorigenic potential of viral latent genes. Cancer Cell *3*, 23–36.

Montaner, S., Sodhi, A., Ramsdell, A.K., Martin, D., Hu, J., Sawai, E.T., and Gutkind, J.S. (2006). The Kaposi's sarcoma-associated herpesvirus G protein-coupled receptor as a therapeutic target for the treatment of Kaposi's sarcoma. Cancer Res. *66*, 168–174.

Moore, P.S., Boshoff, C., Weiss, R.A., and Chang, Y. (1996). Molecular mimicry of human cytokine and cytokine response pathway genes by kshv. Science *274*, 1739–1744.

Moses, A.V., Fish, K.N., Ruhl, R., Smith, P.P., Strussenberg, J.G., Zhu, L., Chandran, B., and Nelson, J.A. (1999). Long-term infection and transformation of dermal microvascular endothelial cells by human herpesvirus 8. J. Virol. *73*, 6892–6902.

Muralidhar, S., Pumfery, A.M., Hassani, M., Sadaie, M.R., Azumi, N., Kishishita, M., Brady, J.N., Doniger, J., Medveczky, P., and Rosenthal, L.J. (1998). Identification of kaposin (open reading frame K12) as a human herpesvirus 8 (Kaposi's sarcoma-associated herpesvirus) transforming gene. J. Virol. *72*, 4980–4988.

Nakamura, H., Li, M., Zarycki, J., and Jung, J.U. (2001). Inhibition of p53 tumor suppressor by viral interferon regulatory factor. J. Virol. *75*, 7572–7582.

Naranatt, P.P., Krishnan, H.H., Svojanovsky, S.R., Bloomer, C., Mathur, S., and Chandran, B. (2004). Host gene induction and transcriptional reprogramming in Kaposi's sarcoma-associated herpesvirus (KSHV/HHV-8)-infected endothelial, fibroblast, and B cells: insights into modulation events early during infection. Cancer Res. *64*, 72–84.

Nicholas, J., Ruvolo, V.R., Burns, W.H., Sandford, G., Wan, X.Y., Ciufo, D., Hendrickson, S.B., Guo, H.G., Hayward, G.S., and Reitz, M.S. (1997). Kaposis sarcoma-associated human herpesvirus-8 encodes homologues of macrophage inflammatory protein-1 and interleukin-6. Nat. Med. *3*, 287–292.

Nicolaides, A., Huang, Y.Q., Li, J.J., Zhang, W.G., and Friedman-Kien, A.E. (1994). Gene amplification and multiple mutations of the K-ras oncogene in Kaposi's sarcoma. Anticancer Res. *14*, 921–926.

Pantanowitz, L., and Dezube, B.J. (2004). Advances in the pathobiology and treatment of Kaposi sarcoma. Curr. Opin. Oncol. *16*, 443–449.

Parsons, C.H., Adang, L.A., Overdevest, J., O'Connor, C.M., Taylor, J.R., Jr., Camerini, D., and Kedes, D.H. (2006). KSHV targets multiple leukocyte lineages during long-term productive infection in NOD/SCID mice. J. Clin. Invest. *116*, 1963–1973.

Pillay, P., Chetty, R., and Reddy, R. (1999). Bcl-2 and p53 immunoprofile in Kaposi's sarcoma. Pathol. Oncol. Res. *5*, 17–20.

Rabkin, C.S., Janz, S., Lash, A., Coleman, A.E., Musaba, E., Liotta, L., Biggar, R.J., and Zhuang, Z. (1997). Monoclonal origin of multicentric Kaposi's sarcoma lesions. N. Engl. J. Med. *336*, 988–993.

Rafii, S., and Lyden, D. (2003). Therapeutic stem and progenitor cell transplantation for organ vascularization and regeneration. Nat. Med. *9*, 702–712.

Safai, B., Johnson, K.G., Myskowski, P.L., Koziner, B., Yang, S.Y., Winningham-Ruddles, S., Godbold, J.H., and Dupont, B. (1985). The natural history of Kaposi's sarcoma in Acquired Immunodeficiency Syndrome. Ann. Intern. Med. *103*, 744–750.

Sherr, C.J., and DePinho, R.A. (2000). Cellular senescence: mitotic clock or culture shock? Cell *102*, 407–410.

Skobe, M., Brown, L.F., Tognazzi, K., Ganju, R.K., Dezube, B.J., Alitalo, K., and Detmar, M. (1999). Vascular endothelial growth factor-C (VEGF-C) and its receptors KDR and flt-4 are expressed in AIDS-associated Kaposi's sarcoma. J. Invest. Dermatol. *113*, 1047–1053.

Staskus, K.A., Zhong, W., Gebhard, K., Herndier, B., Wang, H., Renne, R., Beneke, J., Pudney, J., Anderson, D.J., Ganem, D., and Haase, A.T. (1997). Kaposi's sarcoma-associated herpesvirus gene expression in endothelial (spindle) tumor cells. J. Virol. *71*, 715–719.

Staudt, M.R., Kanan, Y., Jeong, J.H., Papin, J.F., Hines-Boykin, R., and Dittmer, D.P. (2004). The tumor microenvironment controls primary effusion lymphoma growth in vivo. Cancer Res. *64*, 4790–4799.

Wang, H.W., Trotter, M.W., Lagos, D., Bourboulia, D., Henderson, S., Makinen, T., Elliman, S., Flanagan, A.M., Alitalo, K., and Boshoff, C. (2004). Kaposi sarcoma herpesvirus-induced cellular reprogramming contributes to the lymphatic endothelial gene expression in Kaposi sarcoma. Nat. Genet. *36*, 687–693.

Wang, L., Dittmer, D.P., Tomlinson, C.C., Fakhari, F.D., and Damania, B. (2006). Immortalization of primary endothelial cells by the K1 protein of Kaposi's sarcoma-associated herpesvirus. Cancer Res. *66*, 3658–3666.

Yang, T., Chen, S., Leach, M.W., Manfra, D., Homey, B., Wiekowski, M., Sullivan, L., Jenh, C., Narula, S., Chensue, S., and Lira, S.A. (2000). Transgenic expression of the chemokine receptor encoded by HHV8 induces an angioproliferative disease resembling Kaposi's sarcoma. J. Exp. Med. *191*, 445–454.

Zhou, F.C., Zhang, Y.J., Deng, J.H., Wang, X.P., Pan, H.Y., Hettler, E., and Gao, S.J. (2002). Efficient infection by a recombinant Kaposi's sarcoma-associated herpesvirus cloned in a bacterial artificial chromosome: application for genetic analysis. J. Virol. *76*, 6185–6196.

Accession Numbers

The microarray data can be accessed from NCBI's Gene Expression Omnibus (GEO) with accession number GSE6482.